Published in final edited form as:
Curr Biol. 2010 March 9; 20(5): 435–440. doi:10.1016/j.cub.2009.12.062.

Tubulin Glutamylation Regulates Ciliary Motility by Altering Inner Dynein Arm Activity

Swati Suryavanshi[1], **Bernard Eddé**[2], **Laura A. Fox**[3], **Stella Guerrero**[1], **Robert Hard**[4], **Todd Hennessey**[4], **Amrita Kabi**[5], **David Malison**[1], **David Pennock**[5], **Winfield S. Sale**[3], **Dorota Wloga**[1], and **Jacek Gaertig**[1]

[1] Department of Cellular Biology, University of Georgia, Athens, GA 30602

[2] Centre de Recherches de Biochimie Macromoléculaire, CNRS, 34293 Montpellier, France; Université Paris 6, 75252

[3] Department of Cell Biology, Emory University School of Medicine, Atlanta, GA 30322

[4] Department of Biological Sciences, State University of New York, NY 14260

[5] Department of Zoology, Miami University, Oxford, Ohio 45056

SUMMMARY

How microtubule-associated motor proteins are regulated is not well understood. A potential mechanism for spatial regulation of motor proteins is provided by post-translational modifications of tubulin subunits that form patterns on microtubules. Glutamylation is a conserved tubulin modification [1] that is enriched in axonemes. The enzymes responsible for this PTM, glutamic acid ligases (E-ligases), belong to a family of proteins with a tubulin tyrosine ligase (TTL) homology domain (TTL-like or TTLL proteins) [2]. We show that in cilia of *Tetrahymena*, TTLL6 E-ligases generate glutamylation mainly on the B-tubule of outer doublet microtubules, the site of force production by ciliary dynein. Deletion of two TTLL6 paralogs caused severe deficiency in ciliary motility associated with abnormal waveform and reduced beat frequency. In isolated axonemes with a normal dynein arm composition, TTLL6 deficiency did not affect the rate of ATP-induced doublet microtubule sliding. Unexpectedly, the same TTLL6 deficiency increased the velocity of microtubule sliding in axonemes that also lack outer dynein arms, in which forces are generated by inner dynein arms. We conclude that tubulin glutamylation on the B-tubule inhibits the net force imposed on sliding doublet microtubules by inner dynein arms.

RESULTS AND DISCUSSION

TTLL6 enzymes generate tubulin polyglutamylation in cilia

The genome of *Tetrahymena* contains 6 genes encoding TTLL6 paralogs, namely, Ttll6Ap through Ttll6Fp (Fig. 1A). Ttll6Ap is targeted to cilia [2,3]. To characterize the enzymatic properties of Ttll6Ap, we overexpressed GFP-Ttll6Ap in *Tetrahymena*, partially purified and assayed the enzyme for glutamylation of microtubules *in vitro*. Glutamylation involves two distinct steps: initiation and elongation. To distinguish between the two reactions, we used microtubules with varying levels of pre-existing glutamylation: high (adult murine brain tubulin), intermediate (young murine brain tubulin) and low (HeLa tubulin) [4].

Enriched GFP-Ttll6Ap strongly modified microtubules made of adult brain tubulin, less efficiently microtubules made of young brain tubulin, and failed to detectably modify microtubules made of HeLa tubulin (Fig. 1B). The activity was primarily on β-tubulin as seen earlier [2]. Moreover, enriched GFP-Ttll6Ap did not modify unpolymerized adult brain tubulin (Fig. 1B). As a control, we used another partially purified E-ligase, Ttll1p, [5] with the same microtubule substrates, and detected a distinct enzymatic profile (Fig. 1B). These and earlier studies [3,6] are consistent with Ttll6Ap acting primarily as a glutamyl side chain elongase for β-tubulin in microtubules.

In *Tetrahymen*a, glutamylation occurs on most types of microtubules, but the length of the glutamyl side chain is spatially regulated [5], presumably by localized activities of elongases such as Ttll6Ap. While the modification is detectable on most if not all microtubules, only microtubules of cilia and basal bodies are labeled by the polyE antibodies that recognize elongated (poly)glutamyl side chains ([5] and Fig. 1D′). Knocking out the *TTLL6A* gene by DNA homologous recombination neither changed the levels of tubulin glutamylation (Fig. 1C) nor affected the gross phenotype. *TTLL6F* encodes a close paralog (Fig. 1A). Cells with a deletion of *TTLL6F* showed no reduction in the levels of tubulin glutamylation (Fig. 1C). However, a double knockout strain, 6AF-KO, had strongly reduced levels of elongated side chains recognized by polyE antibodies (Fig. 1C), indicating that Ttll6Ap and TtllFp act synergistically. Consistent with this result, 2D gel electrophoresis of axonemal proteins showed a prominent reduction in the abundance of protein isoforms migrating as a smear on the more acidic side of the major β-tubulin spots in 6AF-KO cilia (Fig. S1B). Immunofluorescence with polyE antibodies showed a decrease in tubulin polyglutamylation signal in cilia and basal bodies of 6AF-KO cells imaged side by side with wild type cells (Fig. 1D–D″). The levels of tubulin glutamylation recognized by the GT335 antibody that detects an epitope at the base of the glutamyl side chain and probably recognizes side chains of any length [7] appeared unchanged in 6AF-KO cilia based on immunofluorescence (Fig. 1E–E″, S1A) and western blotting (Fig. 1C). These data indicate that, the absence of Ttll6Ap and Ttll6Fp leads to shortening but not complete loss of glutamyl side chains, which agrees with the enzymatic profile of Ttll6Ap obtained *in vitro*. In cilia of 6AF-KO cells, the levels of tubulin acetylation and glycylation appeared nearly normal (Fig. 1C). Thus, Ttll6Ap and Ttll6Fp together contribute to β-tubulin glutamylation in cilia and are responsible primarily if not exclusively for the chain elongation *in vivo*.

Ttll6Ap and Ttll6Fp affect ciliary motility

The 6AF-KO cells have a normal density of cilia that appear only slightly shorter than wild type cilia (wild type 5.6+/−0.8μm, n = 150; 6AF-KO, 5.0 +/− 0.5 μm, n =150). However, the 6AF-KO cells moved at only 1/5 of wild type rate (Fig 2A). In ciliates, phagocytosis requires the motility of ciliary membranelles that sweep food particles into the oral cavity. Although, the 6AF-KO cells assemble oral membranelles (arrowheads, Fig. 1D,E), they exhibited a greatly reduced rate of formation of food vacuoles (Fig. 2C,D), consistent with malfunction of oral cilia. 6AF-KO cells also showed a reduced rate of multiplication (Fig. 2B). *Tetrahymena* cells require motile cilia for conjugation (our unpublished data). When starved 6AF-KO cells (earlier grown for over 100 generations to reach sexual maturity) were mixed with wild type cells, few pairs formed and these pairs dissociated quickly (Fig. 2E). Thus, all functions dependent on normal ciliary motility appear to be severely affected in 6AF-KO cells.

Biolistic bombardment of 6AF-KO cells with a GFP-Ttll6Ap transgene (targeted to an unrelated locus) resulted in the appearance of cells with vigorous motility (at the frequency of 0.014%), and no such cells were found in the mock-transformed population ($n=10^7$). The rescued cells had a GFP signal in cilia and basal bodies (results not shown) and recovered a nearly normal rate of motility, multiplication (Fig. 2A,B), and phagocytosis (Table S3).

Thus, the dramatic loss of ciliary functions seen in 6AF-KO cells is caused by the loss of TTLL6 protein activity.

High-speed video microscopy showed that in wild type cells, locomotory cilia had an asymmetric waveform and rows of cilia were engaged in metachronal waves (movie S1A, S2A). In contrast, in 6AF-KO cells, many cilia appeared straight and some were seen rotating around a central pivot point, often colliding with each other in an uncoordinated motion (movie S1B). Furthermore, immunofluorescence images indicate that 6AF-KO cilia are more straight than wild type (Fig. 1D,E). In some 6AF-KO cultures grown for over 480 generations, the waveform was partly restored to normal. In these "adapted" 6AF-KO cells (6AF-KO^{A}), the beat frequency could be measured, and was found to be ~ 60% of wild type (Fig. 2F, movie S2B).

Exposure of wild type *Tetrahymena* cells to 20 μg/ml of sodium dodecyl benzene sulfonate (SDBS), causes rapid avoidance reaction associated with backward motility, likely by depolarizing the ciliary plasma membrane (T.H., unpublished data). While wild type cells showed rapid SDBS-induced avoidance responses (based on deviations from the linearity of swimming paths), the 6AF-KO cells failed to swim backwards, and instead slightly increased the rate of forward motility (Fig. 2G,H). The responses of 6AF-KO cells to other plasma membrane-depolarizing treatments (1 mM Ba^{++}, 20 mM Ca^{++}) were similar to SDBS (results not shown). At the time of addition of SDBS, some 6AF-KO cells showed a slight turn (Fig. S2), indicating that the signal detection pathways that regulate motility are at least partly functional. These data suggests that the response to signals, that requires proper modulation of activity of dynein arms, is affected. However, ultrastructural studies revealed that 6AF-KO axoneme cross-sections have a normal morphology (Fig. 3A,B, n=209). No difference was found in the frequency of outer (ODA) and inner dynein arms (IDA) on wild type and 6AF-KO axoneme cross-sections (Fig. 3C). Thus, we considered that TTLL6 enzymes, via tubulin glutamylation, could be affecting the activity ciliary dyneins.

Ttll6Ap and Ttll6Fp primarily modify the B-tubule of outer microtubules

Immunogold TEM studies showed that overexpressed GFP-Ttll6Ap localized to the outer doublets and not to central microtubules in all of cross-sections examined (Fig. 3D,E n=38). We evaluated the distribution of polyglutamylated (polyE) epitopes on isolated doublet microtubules that were extruded from the axoneme with 40 μM ATP (see below). In negatively stained doublet microtubules viewed on edge, the A-tubule can be identified based on its increased width (as compared to the B-tubule), and dynein arms projecting from its surface (arrowhead, Fig. 3G,H). In wild type doublets, the majority of gold particles were detected in proximity of the B-tubule (Fig. 3F,G,S3) and the signal was dramatically reduced in 6AF-KO axonemes (Fig. 3F,H,S3). Thus, Ttll6Ap and TtllFp primarily generate glutamylation on the B-tubule. Our observations are consistent with earlier microscopic and biochemical studies showing enrichment of tubulin glutamylation on the B-tubule [8–10]. Since the B-tubule serves as a track for ciliary dynein, the primary role of tubulin glutamylation in cilia could be to regulate the motor activity of ciliary dynein.

Tubulin glutamylation strongly affects the inner dynein arm-driven microtubule sliding in isolated axonemes *in vitro*

When isolated *Tetrahymena* axonemes are exposed to ATP, outer doublet microtubules undergo unconstrained dynein-driven microtubule sliding (rather than reactivated bending) and the velocity of ATP-induced axonemal microtubule sliding can be used to assay the activity of ciliary dynein *in situ* [11–13]. With 1 mM ATP, microtubules underwent sliding at similar rates in wildtype and 6AF-KO axonemes (Fig. 4B). In wild type axonemes, the

microtubule sliding velocity is believed to be primarily determined by the activity of ODAs (reviewed in [14]). To test whether the TTLL6-mediated tubulin glutamylation affects the microtubule sliding generated specifically by IDAs, we constructed a strain that lacks *TTLL6A* and *TTLL6F* and is homozygous for the temperature-sensitive *oad1-1* allele. When *oad1-1* mutants are grown at restrictive temperature (38°C), ODAs fail to assemble and cells are nearly paralyzed [15,16]. We assessed microtubule sliding in axonemes isolated from wildtype, *oad1-1*, 6AF-KO and 6AF-KO;*oad1-1* triple mutant cells, all grown for 12 hr at 38°C. We confirmed that 6AF-KO;*oad1-1* cells had fewer ODAs as compared to 6AF-KO cells grown at the same temperature (Fig. 4A). As reported [17], *oad1-1* axonemes showed a decreased rate of microtubule sliding as compared to wild type (Fig. 4C) while wild type and 6AF-KO axonemes showed nearly the same microtubule sliding velocity, as seen earlier for axonemes from cells grown at the standard temperature (compare Fig. 4B,C). Unexpectedly, the 6AF-KO;*oad1-1* axonemes showed a nearly two-fold increase in the rate of microtubule sliding as compared to *oad1-1* axonemes (Fig. 4C). These data indicate that tubulin glutamylation generated on the B-tubule by Ttll6Ap and Ttll6Fp has a restraining effect on the microtubule sliding velocity generated by the net activity of IDAs.

To conclude, we report that tubulin polyglutamylation generated by TTLL6 enzymes plays a major role in ciliary motility, and that the mechanism appears to involve regulation of inner dynein arm activity. Earlier studies have implicated tubulin glutamylation in axoneme assembly [18,19]. Deletion of additional TTLL6 paralogs in *Tetrahymena* led to major shortening of the axoneme (our unpublished data). Thus, tubulin glutamylation affects both axoneme assembly and motility and the latter function may require a higher dose of TTLL6 activity. A recent study of a *Chlamydomona*s mutant defective in TTLL9, an α-tubulin-preferring E-ligase, also revealed that tubulin polyglutamylation controls ciliary motility by affecting inner dynein arm activity [20]. Thus, both studies link tubulin glutamylation, mediated by two conserved E-ligases on either α- or β-tubulin, to regulation of IDA activity. The abnormal waveform and lack of ciliary reversals that we observed in the 6AF-KO cells are also consistent with malfunctioning IDAs in *Tetrahymena* [21,22]. The mechanochemical properties of ODAs and IDAs are distinct but the underlying structural basis is not well understood (reviewed in [14]). For example, in *Tetrahymena*, the 22S dynein fraction from the salt extract of axonemes (mainly ODAs) produces a linear gliding of microtubules at the rate of 8 μm/s, while the 14S dynein fraction (presumably IDAs) produces a motility at the rate of 4 μm/s associated with microtubule rotation [23]. Importantly, two IDA subtypes that were studied in *Chlamydomonas* (dynein c and f/I1) display processive movements along microtubules [24,25]. Kotani and colleagues proposed that in the bending cilium, processive IDAs, acting simultaneously with faster ODAs, impose a drag on sliding microtubules and could increase the axoneme curvature [25]. We speculate that tubulin glutamylation is important for the processive motility of IDAs. One unusual feature of dynein motor domain is that it contacts the microtubule track by a conserved stalk domain [26]. Recent studies indicate that the stalk acts as a tether that allows for pulling of parts of the dynein molecule toward the microtubule during the power stroke [27,28]. Thus, tubulin glutamylation could regulate the affinity of the stalk in inner dynein arms to the B-tubule. The patterns of glutamylation vary between axonemes of different species [29]. Thus, specific beating patterns could be dependent on diverse patterns of tubulin glutamylation.

EXPERIMENTAL PROCEDURES

Germ line targeting

To prepare targeting plasmids, fragments of macronuclear DNA of T. *thermophila* were amplified for each locus and subcloned on either side of a selectable drug resistance cassette (Table S1). The targeting fragments were transformed biolistically and knockout strains

were constructed as described in detail in the Supplemental Material. For rescue, vegetatively growing 6AF-KO cells were biolistically transformed with a fragment encoding MTT1-GFP-TTLL6A targeted to *BTU1* [2]. A strain lacking *TTLL6A* and *TTLL6F* and homozygous the *oad1-1* mutation [16] was constructed by standard crosses.

Phenotypic studies

The multiplication, cell motility and phagocytosis rates were measured as described [5]. To assay swimming behavior, 2 ml of cells (2×10^5 cells/ml) were added to 100 ml of wash buffer (10 mM Tris, 50 μM $CaCl_2$, MOPS pH 7.2), centrifuged at 1000 × g for 2 min and suspended in 2 ml. After 30 min of adaptation, cells were assayed in 70 μl drop on a two-ring slide, with or without SDBS (20 μg/ml) and video recordings were done under a dissecting microscope with a Moticam 480 digital camera. To measure the beat frequency, cells (2×10^5 cells/ml) were recorded at 500 frames/sec by a Photronics 1280 PCI FastCam on a Nikon Eclipse E600 microscope. Immunofluorescence and electron microscopy studies were done using standard protocols as described in the Supplemental Material.

Biochemical studies

Partial purifications of Ttll6Ap and Ttll1p from overproducing *Tetrahymena* strains and *in vitro* glutamylation assays with taxotere–stabilized microtubules made of the murine brain and HeLa tubulin were performed as described [5].

To purify cilia, *Tetrahymena* cells were grown to a density of 3×10^5 cells/ml in 500 ml of SPP, washed with 10 mM Tris pH 7.5 and suspended in 40 ml of 10 mM Tris, 50 mM sucrose, 10 mM $CaCl_2$ with protease inhibitors (Complete, Roche). Deciliation was initiated by adding 600 μl of 0.5 M acetic acid, after 2 min followed by 550 μl of 0.6M KOH. Cell bodies were removed (1860 × g, 5 min) and cilia were collected (23,300 × g, 15 min, 4°C) and suspended in 500 μl of the axoneme buffer (20 mM potassium acetate, 5 mM $MgSO_4$, 0.5 mM EDTA, 20 mM HEPES, pH 7.6).

Microtubule sliding in isolated axonemes

Cilia were suspended at 0.1 mg protein/ml in the axoneme buffer (without protease inhibitors). For experiments on axonemes purified from strains carrying the *oad1-1* mutation, all strains were grown for 12 hr at 38°C with inocula adjusted according to individual growth rates to collect cells at 3×10^5 cells/ml. Cilia were suspended at 0.1 mg protein/ml in 500 μl of the motility buffer (1mM DTT, 50 mM potassium acetate, 5 mM MgSO4, 1mM EGTA, 30 mM HEPES, PEG 1%, pH 7.6). To demembranate, 10 μl of 1% NP-40 in motility buffer was added to 50 μl of diluted cilia. The axoneme suspension was pipetted into a perfusion chamber constructed with a glass slide and cover slip separated by double stick tape. The perfusion chamber was washed with 50 μl of axoneme buffer followed by perfusion with 50 μl of 1 mM of ATP, in the motility buffer. The sliding of microtubules was recorded on a Zeiss Axiovert 35 microscope equipped with dark field optics (40 X PlanApo), on a silicon-intensified camera (VE-1000, Dage-MTI, Michigan City, IN). The video images were converted to a digital format using Labview 7.1 software (National Instruments, Austin, TX). The sliding velocity was determined manually by measuring microtubule end displacement, as a function of time, on tracings calibrated with a micrometer [12].

Supplementary Material

Refer to Web version on PubMed Central for supplementary material.

Acknowledgments

We are grateful to Ritsu Kamiya (University of Tokyo) for sharing results prior to publication. This study was supported by grants from the NSF (MBC-033965 to JG) and NIH (R37 GM51173 to W.S.S). We thank the following researchers for providing reagents: Jody Bowen and Martin A. Gorovsky (University of Rochester) for polyE, polyG and SG antibodies and the rpl29 cassette, Joseph Frankel (University of Iowa) for 12G10 mAb (available from the DSHB) and Paul Doerder (Cleveland State University) for SerH antibodies. We acknowledge the excellent technical assistance with TEM by Mary Ard.

References

1. Edde B, Rossier J, Le Caer JP, Desbruyeres E, Gros F, Denoulet P. Posttranslational glutamylation of alpha-tubulin. Science 1990;247:83–85. [PubMed: 1967194]
2. Janke C, Rogowski K, Wloga D, Regnard C, Kajava AV, Strub JM, Temurak N, van Dijk J, Boucher D, van Dorsselaer A, et al. Tubulin polyglutamylase enzymes are members of the TTL domain protein family. Science 2005;308:1758–1762. [PubMed: 15890843]
3. Wloga D, Dave D, Meagley J, Rogowski K, Jerka-Dziadosz M, Gaertig J. Hyperglutamylation of tubulin can either stabilize or destabilize microtubules in the same cell. Eukaryot Cell. 2009
4. Regnard C, Fesquet D, Janke C, Boucher D, Desbruyeres E, Koulakoff A, Insina C, Travo P, Edde B. Characterisation of PGs1, a subunit of a protein complex co-purifying with tubulin polyglutamylase. J Cell Sci 2003;116:4181–4190. [PubMed: 12972506]
5. Wloga D, Rogowski K, Sharma N, Van Dijk J, Janke C, Edde B, Bre MH, Levilliers N, Redeker V, Duan J, et al. Glutamylation on alpha-tubulin is not essential but affects the assembly and functions of a subset of microtubules in Tetrahymena thermophila. Eukaryot Cell 2008;7:1362–1372. [PubMed: 18586949]
6. van Dijk J, Rogowski K, Miro J, Lacroix B, Edde B, Janke C. A targeted multienzyme mechanism for selective microtubule polyglutamylation. Mol Cell 2007;26:437–448. [PubMed: 17499049]
7. Wolff A, de Nechaud B, Chillet D, Mazarguil H, Desbruyeres E, Audebert S, Edde B, Gros F, Denoulet P. Distribution of glutamylated alpha and beta-tubulin in mouse tissues using a specific monoclonal antibody, GT335. Eur J Cell Biol 1992;59:425–432. [PubMed: 1493808]
8. Kann ML, Prigent Y, Fouquet JP. Differential distribution of glutamylated tubulin in the flagellum of mouse spermatozoa. Tissue Cell 1995;27:323–329. [PubMed: 7645010]
9. Lechtreck KF, Geimer S. Distribution of polyglutamylated tubulin in the flagellar apparatus of green flagellates. Cell Motil Cytoskeleton 2000;47:219–235. [PubMed: 11056523]
10. Multigner L, Pignot-Paintrand I, Saoudi Y, Job D, Plessmann U, Rudiger M, Weber K. The A and B tubules of the outer doublets of sea urchin sperm axonemes are composed of different tubulin variants. Biochemistry 1996;35:10862–10871. [PubMed: 8718878]
11. Summers KE, Gibbons IR. Adenosine triphosphate-induced sliding of tubules in trypsin-treated flagella of sea-urchin sperm. Proc Natl Acad Sci U S A 1971;68:3092–3096. [PubMed: 5289252]
12. Okagaki T, Kamiya R. Microtubule sliding in mutant Chlamydomonas axonemes devoid of outer or inner dynein arms. J Cell Biol 1986;103:1895–1902. [PubMed: 2946702]
13. Sale WS, Satir P. Direction of active sliding of microtubules in Tetrahymena cilia. Proc Natl Acad Sci U S A 1977;74:2045–2049. [PubMed: 266725]
14. Kamiya R. Functional diversity of axonemal dyneins as studied in Chlamydomonas mutants. Int Rev Cytol 2002;219:115–155. [PubMed: 12211628]
15. Ludmann SA, Schwandt A, Kong X, Bricker CS, Pennock DG. Biochemical analysis of a mutant Tetrahymena lacking outer dynein arms. J Eukaryot Microbiol 1993;40:650–660. [PubMed: 8401477]
16. Attwell GJ, Bricker CS, Schwandt A, Gorovsky MA, Pennock DG. A temperature-sensitive mutation affecting synthesis of outer arm dyneins in Tetrahymena thermophila. J Protozool 1992;39:261–266. [PubMed: 1533674]
17. Seetharam RN, Satir P. High speed sliding of axonemal microtubules produced by outer arm dynein. Cell Motil Cytoskeleton 2005;60:96–103. [PubMed: 15605357]
18. Campbell PK, Waymire KG, Heier RL, Sharer C, Day DE, Reimann H, Jaje JM, Friedrich GA, Burmeister M, Bartness TJ, et al. Mutation of a novel gene results in abnormal development of

spermatid flagella, loss of intermale aggression and reduced body fat in mice. Genetics 2002;162:307–320. [PubMed: 12242242]

19. Pathak N, Obara T, Mangos S, Liu Y, Drummond IA. The zebrafish fleer gene encodes an essential regulator of cilia tubulin polyglutamylation. Mol Biol Cell 2007;18:4353–4364. [PubMed: 17761526]
20. Kubo T, Haru-aki Y, Yagi T, Hirono M, Kamiya R. Tubulin polyglutamylation regulates axonemal motility by changing activities of inner arm dyneins. 2009 Submitted.
21. Wood CR, Hard R, Hennessey TM. Targeted gene disruption of dynein heavy chain 7 of Tetrahymena thermophila results in altered ciliary waveform and reduced swim speed. J Cell Sci 2007;120:3075–3085. [PubMed: 17684060]
22. Hennessey TM, Kim DY, Oberski DJ, Hard R, Rankin SA, Pennock DG. Inner arm dynein 1 is essential for Ca++-dependent ciliary reversals in Tetrahymena thermophila. Cell Motil Cytoskeleton 2002;53:281–288. [PubMed: 12378538]
23. Vale RD, Toyoshima YY. Rotation and translocation of microtubules in vitro induced by dyneins from Tetrahymena cilia. Cell 1988;52:459–469. [PubMed: 2964278]
24. Sakakibara H, Kojima H, Sakai Y, Katayama E, Oiwa K. Inner-arm dynein c of Chlamydomonas flagella is a single-headed processive motor. Nature 1999;400:586–590. [PubMed: 10448863]
25. Kotani N, Sakakibara H, Burgess SA, Kojima H, Oiwa K. Mechanical properties of inner-arm dynein-f (dynein I1) studied with in vitro motility assays. Biophys J 2007;93:886–894. [PubMed: 17496036]
26. Gee MA, Heuser JE, Vallee RB. An extended microtubule-binding structure within the dynein motor domain. Nature 1997;390:636–639. [PubMed: 9403697]
27. Ueno H, Yasunaga T, Shingyoji C, Hirose K. Dynein pulls microtubules without rotating its stalk. Proc Natl Acad Sci U S A 2008;105:19702–19707. [PubMed: 19064920]
28. Carter AP, Garbarino JE, Wilson-Kubalek EM, Shipley WE, Cho C, Milligan RA, Vale RD, Gibbons IR. Structure and functional role of dynein's microtubule-binding domain. Science 2008;322:1691–1695. [PubMed: 19074350]
29. Hoyle HD, Turner FR, Raff EC. Axoneme-dependent tubulin modifications in singlet microtubules of the Drosophila sperm tail. Cell Motil Cytoskeleton 2008;65:295–313. [PubMed: 18205200]

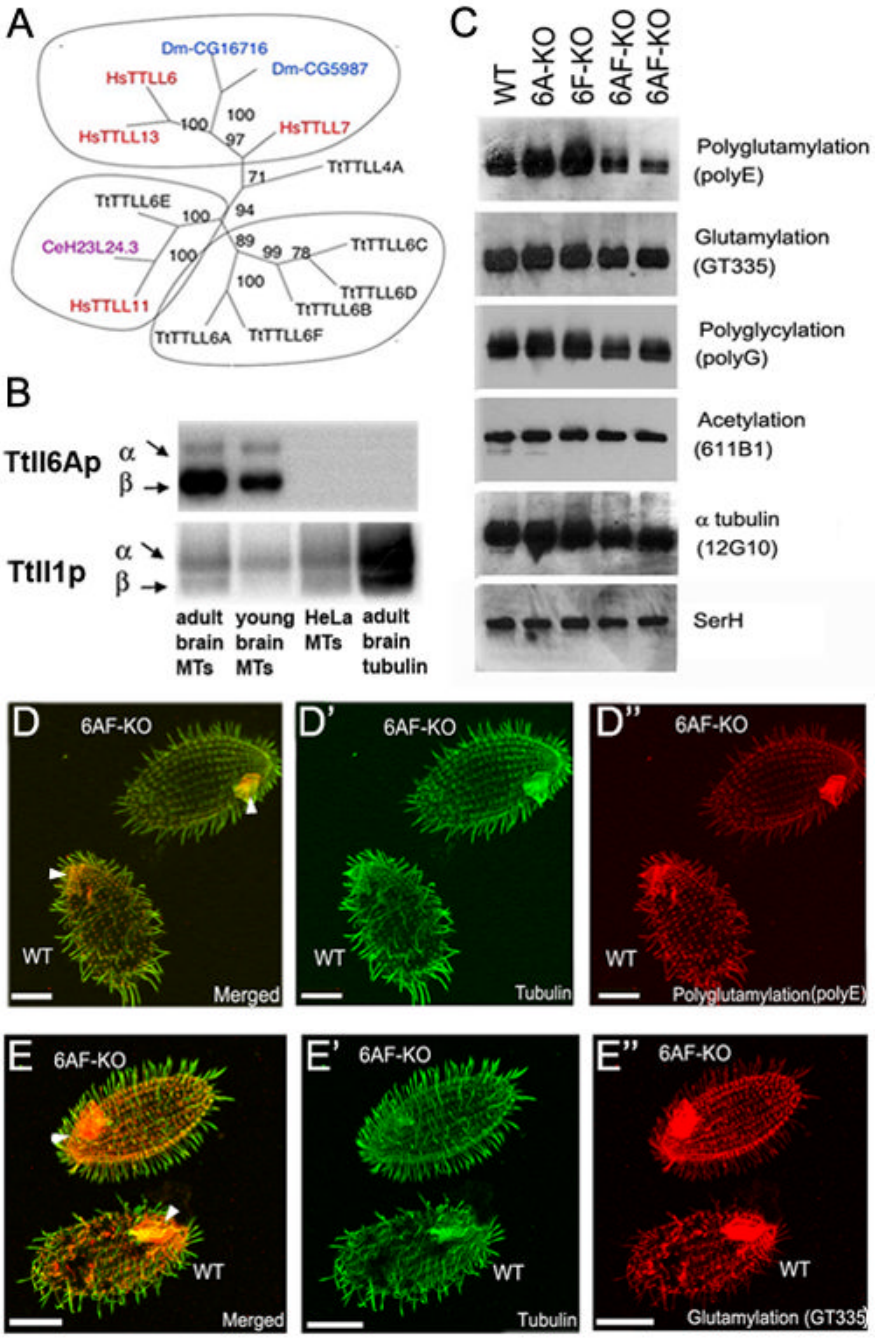

Figure 1. Deletion of Ttll6Ap and Ttll6Fp leads to a loss of tubulin glutamylation in cilia

(A) A neighbor-joining phylogenetic tree based on the catalytic domain of TTLL6 E-ligases [5]. Tt-Ttll4Ap was used as an outgroup. Abbreviations of species: Hs, *Homo sapiens*; Ce, *Caenorhabditis elegans*; Dm, *Drosophila melanogaster*; Tt, *Tetrahymena thermophila*. (B) A fluorogram of mammalian microtubule proteins (20 μg) separated by SDS-PAGE after *in vitro* glutamylation with partially purified GFP-Ttll6Ap and GFP-Ttll1p, ATP and ^{3}H-glutamate. (C) A western blot of cilia proteins. The anti-SerH antigen antibodies were used as a loading control. (D–E″) Immunofluorescence images of pairs of wildtype and 6AF-KO cells imaged side by side. Wildtype cells were prefed with India Ink to reveal dark food vacuoles. Cells were labeled with 12G10 anti-α-tubulin mAb and polyE anti-

polyglutamylation antibodies (D–D″) or with SG anti-total tubulin antibodies and GT335 anti-glutamylated tubulin mAb (E–E″). Arrowheads mark oral membranelles. Bar = 10 μm. Quantitative data are shown in Fig. S1A.

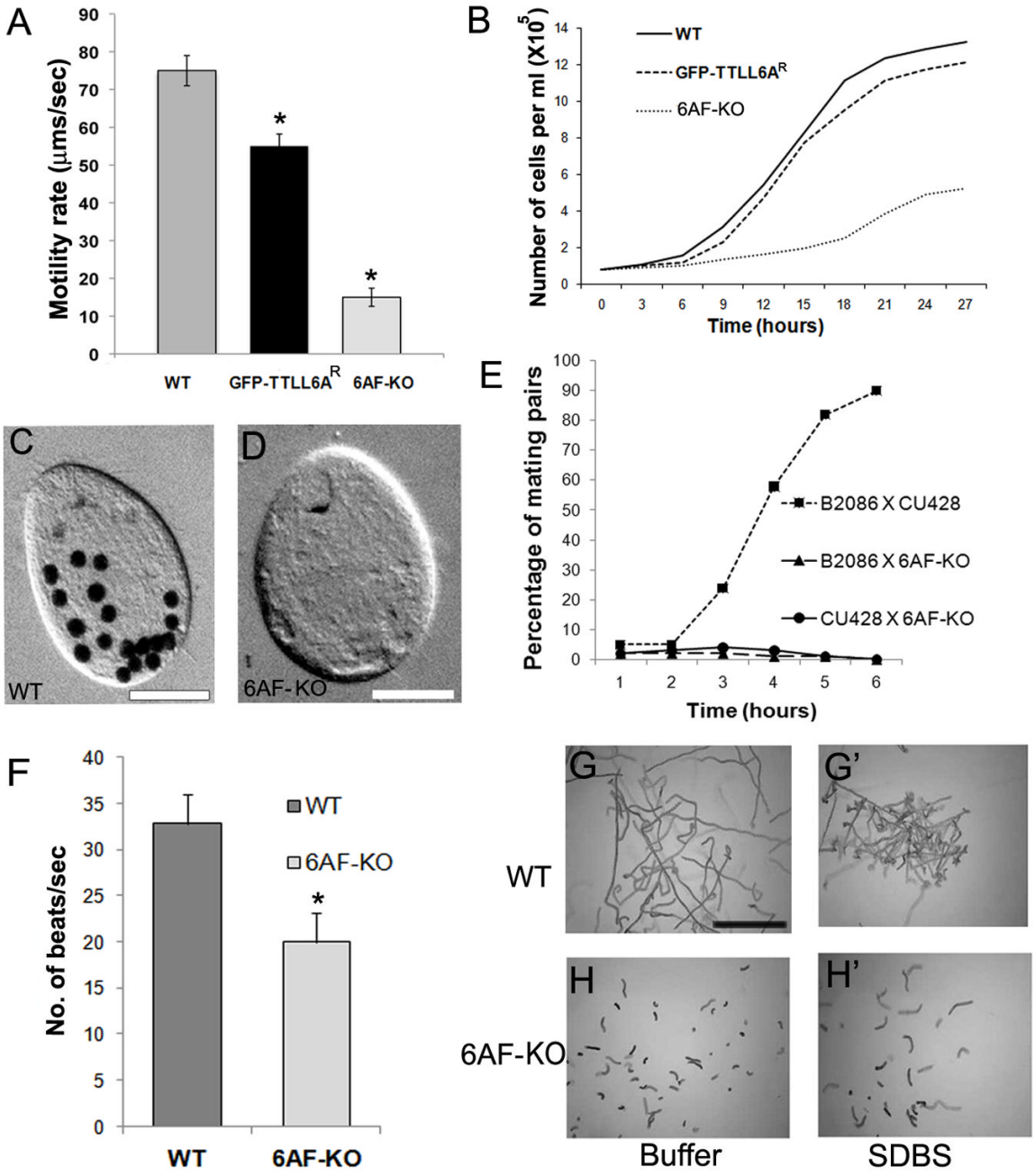

Figure 2. Cells lacking Ttll6Ap and Ttll6Fp display a loss of cilia-dependent functions

(A) A histogram shows the average linear cell motility rate during 5 sec for wild type, 6AF-KO and 6AF-KO cells rescued with a GFP-Ttll6Ap transgene (6AF-KO^R) (n=40 for each strain). Bars represent standard deviations. *p<0.001. (B) Culture growth curves. (C–D) Images of a wild type (C) and 6AF-KO (D) cell exposed to India ink for 30 min. Bar = 20 μm. (E) The graph shows the percentage of paired cells following mixing of either two starved wild type strains (CU428 and B2086) or 6AF-KO cells with either of the two wild type strains. (F) The average ciliary beat frequency for wild type (n=27) and 6AF-KO cells (n=27, p<0.0001). Error bars represent standard deviations. (G–H′). Swimming responses to SDBS. Wild type (G–G′) or 6AF-KO (H–H′) cells were exposed to either a buffer alone or SDBS (20 μg/ml), and the paths of live cells were recorded for 1 sec. Bar = 1 mm.

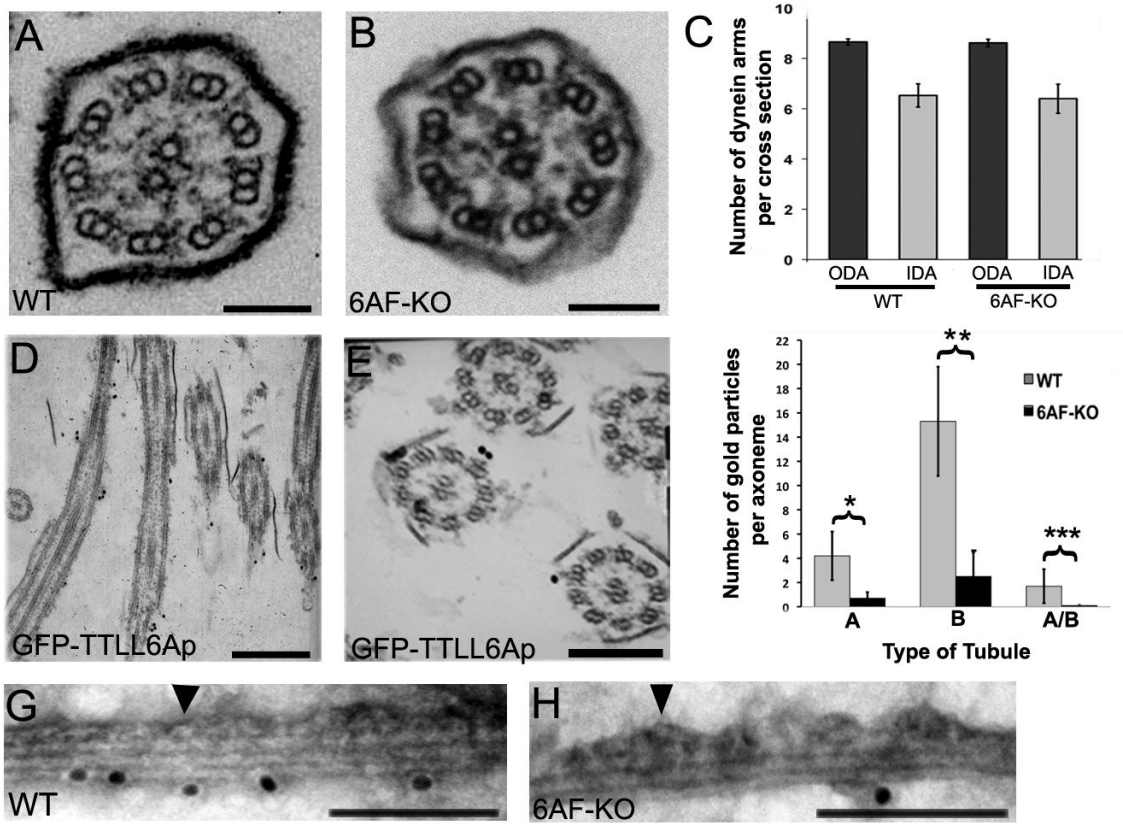

Figure 3. Ttll6Ap and Ttl6Fp generate polyglutamylation primarily on B-tubule of outer microtubules

(A–B) Cross sections of wild type (A) and 6AF-KO (B) cilia of cells grown at 30°C. Bar = 100 nm (C) A graph that documents the average number of IDAs and ODAs per axoneme cross-section (wild type n= 27; 6AF-KO n= 27). Error bars represent standard errors. (D–E) Sections of cells expressing GFP-Ttll6Ap that were labeled with anti-GFP antibodies using immunogold TEM. Bar in D = 750 nm. Bar in E = 250 nm. (F) A graph that quantifies the localization of polyglutamylated tubulin epitopes in doublet microtubules labeled by whole mount immunogold microscopy (shown in Fig. 3G, H and Fig. S3) using polyE antibodies and anti-rabbit IgG 10 nm gold conjugates. Each gold particle was scored as associated more closely with either the A- or B-tubule, or the inter-tubule junction (A/B). Error bars represent standard deviations. *p=0.0001, **p<0.0001, ***p=0.0085. Twelve wild type and 12 6AF-KO axonemes were scored (G, H) Examples of isolated doublet microtubules of wild type (G) and 6AF-KO origin (H) analyzed by whole mount immunogold microscopy using polyE antibodies. Arrowheads mark the A-tubule covered with dynein arms. Additional images are shown in Fig. S3. Bar = 100 nm.

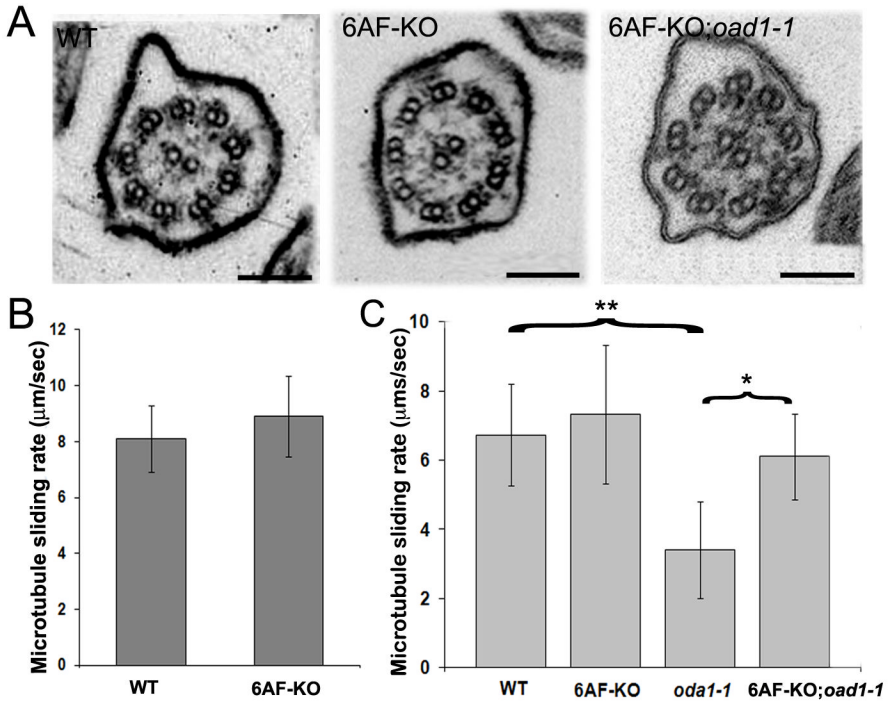

Figure 4. Tubulin glutamylation regulates the velocity of inner dynein arm driven microtubule sliding in axonemes *in vitro*

(A) TEM cross-sections of wildtype, 6AF-KO and 6AF-KO;*oad1* axonemes grown for 12 hr at 38°C. Bar = 125 nm. The average numbers of dynein arms on scored axoneme cross-sections were as follows: 6AF-KO: 8.6 +/− 0.2 ODA, 6.4 +/− 0.6 IDA per section, n=15; 6AF-KO;*oad1-1*: 2.8 +/− 0.5 ODA, 6.5 +/− 0.2 IDA per section, n=15. (B) A graph shows the average sliding velocity of wild type (n=40) and 6AF-KO (n=40) axonemes obtained from cells grown at the standard temperature (30°C). Error bars represent standard deviations. Data were collected in 3 independent experiments. (C) A graph that documents the average sliding velocity of wild type (n=74), *oad1-1* (n=41) 6AF-KO (n=73), and 6AF-KO;*oad1-1* (n=46) axonemes obtained from cells grown at the 38°C, to induce the loss of ODAs in cells that are homozygous for the *oad1-1* allele. Error bars represent standard deviations. *p<0.0001 for 6AF-KO;*oad1-1* vs wildtype; **p<0.0001 for *oad1-1* vs wildtype. Data were collected in 3 independent experiments.